Accurate 3-D Localization of Selected Smart Objects in Optical Internet of Underwater Things

Nasir Saeed, *Senior Member, IEEE*, Mohamed-Slim Alouini, *Fellow, IEEE*, and Tareq Y. Al-Naffouri, *Senior Member, IEEE*

***Abstract*—Localization is a fundamental task for the optical Internet of Underwater Things (O-IoUT) to enable various applications, such as data tagging, routing, navigation, and maintaining link connectivity. The accuracy of the localization techniques for O-IoUT greatly relies on the location of the anchors. Therefore, recently, the localization techniques for O-IoUT which optimize the anchor's location have been proposed. However, the optimization of the anchors' location for all the smart objects in the network is not a useful solution. Indeed, in a network of densely populated smart objects, the data collected by some sensors are more valuable than the data collected from other sensors. Therefore, in this article, we propose a 3-D accurate localization technique by optimizing the anchor's location for a set of smart objects. Spectral graph partitioning is used to select the set of valuable sensors. The numerical results show that the proposed technique of optimizing anchor's location for a set of selected sensors provides a better location accuracy.**

***Index Terms*—Anchor's location, data tagging, localization, optical Internet of Underwater Things (O-IoUT), routing.**

I. Introduction

OCEANS hold 96% of the earth's water which nurtures life on this planet and regulates its climate. Therefore, it is essential to keep track of the change in oceans and to investigate its unexplored regions for the benefits of humankind. In the past decade, there has been an increasing demand for underwater applications, such as environmental monitoring, coastal surveillance, navigation, and underwater exploration. These applications can be accomplished by using Internet of Underwater Things (IoUT) [1].

Apparently, efficient communication between different entities of an IoUT network is a fundamental and critical issue. Existing IoUT networks use radio frequency (RF), acoustic, and optical waves for information transmission [2]. Each of these communication sources has advantages and disadvantages. RF waves are highly absorbed in aquatic medium and therefore can only be used on the surface of the water. On the contrary, acoustic waves attain longer transmission ranges, but due to the low speed of sound waves, it has high latency and low data rate. Recently, optical waves have emerged as a good alternative to its counterpart RF and acoustic waves, due to its ability to provide high-speed underwater communication [3]. However, the transmission range of optical waves is in tens of meters, which is low as compared to acoustic waves. The transmission range of underwater optical wireless communication (UOWC) is limited due to the intrinsic properties of light and different propagation losses in water, such as absorption, scattering, turbulence, and salinity. Due to the aforementioned limitations of UOWC, a dense network deployment of the smart objects is required in optical IoUT (O-IoUT) to traverse the information through the network in a multihop fashion [4].

Moreover, numerous applications of O-IoUT, such as navigation, surveillance, data tagging, and routing require location information of the deployed smart objects. In the past, a large number of localization techniques have been proposed for IoUT networks based on acoustic waves [5], [6]. However, few works exist on locating the underwater smart objects operating on optical waves. For example, Akhoundi *et al.* [7] proposed a time of arrival (ToA) and received signal strength (RSS)-based positioning techniques for O-IoUT. However, in this article, the authors assumed that underwater optical smart objects directly communicate with the beacons which may not be practical due to the limited transmission range of UOWC links. Hence, in [8]–[11], various multihop localization techniques were introduced for smart objects operating on optical waves.

Nonetheless, the localization of the underwater smart objects is greatly influenced by the location of anchors. Therefore, the research community on localization came up with different techniques to improve the localization accuracy of a single smart object by optimizing the location of anchors [12], [13]. However, a few works exist on optimizing the location of anchors to reduce the localization error of all smart objects in the network [14]. Recently, Saeed *et al.* [11] proposed a 3-D localization technique for O-IoUT which accounts for the outliers in range measurements and optimizes the anchor's location. However, the optimization of the anchors' location for all the smart objects in the network may not be a useful solution.

Indeed, in large-scale O-IoUT networks, efficient collection of the data is an important task. These large-scale networks allow us to get a large amount of data, however, it is not always desirable from various perspectives, such as processing time, network lifetime, communication overhead, and available storage. Besides, authentication of the smart objects is

Manuscript received September 15, 2019; accepted October 5, 2019. Date of publication October 8, 2019; date of current version February 11, 2020. This work was supported by the Office of Sponsored Research at King Abdullah University of Science and Technology. *(Corresponding author: Nasir Saeed.)*

The authors are with the Department of Electrical Engineering, Computer Electrical and Mathematical Sciences and Engineering Division, King Abdullah University of Science and Technology, Thuwal 23955-6900, Saudi Arabia (e-mail: mr.nasir.saeed@ieee.org).

Digital Object Identifier 10.1109/JIOT.2019.2946270

also required for security of the network [15]. Additionally, in such networks, the data collected by some smart objects may be more important as compared to the data collected from the other smart objects depending on the application scenario. For example, in an application of surveillance or intruder detection, the information from the smart objects which detect the intruder is more important than the other smart objects. Therefore, it is more crucial to find the location of valuable smart objects more accurately compared to other smart objects in such networks. Hence, in this article, we propose a 3-D accurate localization technique by selecting the set of vital smart objects and optimizing the anchors' location for these smart objects. The contributions of this article are summarized as follows.

1) A joint smart object selection and 3-D localization problem for O-IoUT is formulated as a network graph. If the surface buoys, which are also acting as anchors, are located at the surface only, the localization problem in 3-D cannot be solved regardless of the number of surface buoys deployed. Hence, we consider smart self-propelled surface buoys that can move on the surface of the water as well as can dive and rise to the surface. We have shown that the optimization of anchors for a specific set of smart objects is a good strategy to improve their localization accuracy.
2) A graph partitioning technique is used to divide the network into a disjoint set of graphs where each of the disjoint graphs represents a set of smart objects.
3) The localization accuracy of the selected smart objects is improved by optimizing the anchors' location for the specific set of smart objects instead of the whole network. Moreover, the numerical results show that localization accuracy also depends on the transmission range, ranging error, number of anchors, and density of the smart objects. The proposed method can be applied to both large-scale and small-scale networks satisfying the condition of connectivity.

The remainder of this article is organized as follows. Related work is reviewed in Section II. Problem formulation and proposed localization technique are presented in Sections III and IV, respectively. Sections V and VI provide the simulation results and conclusions, respectively.

II. Related Work

This section covers the literature on localization techniques for O-IoUT. Location-based services can provide many solutions to the future smart world, such as smart agriculture, smart cities, smart oceans, etc. Therefore, the localization for various terrestrial networks is widely studied, which mainly relies on the global positioning system (GPS), cellular positioning systems, and indoor positioning systems. For instance, Shit *et al.* [16] proposed a probabilistic RSS-based fingerprinting localization for terrestrial IoT networks. Quite a good number of review articles are presented on localization for the terrestrial networks. For instance, Shit *et al.* [17] reviewed a large number of localization techniques for small word applications. Similarly, the importance of localization and taxonomy of localization techniques for IoT networks are presented in [18]. However, most of these works are focused on localization for terrestrial IoT networks which mainly uses electromagnetic waves, and therefore, may not be applicable in the marine environment. Hence, acoustic waves-based positioning systems, such as short baseline and long baseline are developed for the underwater environment. A large number of underwater localization algorithms have been proposed in the past for underwater acoustic wireless communication systems. All of these localization algorithms consider different parameters of the network, such as network topology, range measurement technique, energy requirement, and device capabilities. In addition, the accuracy of localization algorithms also depends on many other factors, which include propagation losses, number of anchor nodes, location of anchor nodes, time synchronization, and scheduling. The underwater localization algorithms can be classified based on different parameters, such as range-based/range-free, anchor-based/anchor-free, stationary/mobile, and centralized/distributed [19]. Based on the motion capabilities of the anchors, there are two major categories. First is the nonpropelled anchors which can be stationary or floats freely on the surface of the water while the second type is propelled anchors which are equipped with inertial navigation systems and can move on the surface as well as underwater. Examples of nonpropelled anchors include floaters and gliders while propelled anchors include AUVs and submarines. For instance, in [20], the idea of anchors with vertical mobility was introduced. The anchors were supported mechanically by detachable elevator transceivers to move up and down in the underwater environment. A similar approach was also used in [21] for underwater acoustic sensor networks localization with ToA ranging. A propelled approach with AUV as an anchor was used in [22] and [23] to localize the underwater sensors. The AUV-based approach requires two-way ranging and perfect synchronization. A dive and rise localization technique was introduced in [24], where the anchors were able to descend and ascend in the underwater environment. The dive and rise approach was further extended in [25], where the underwater nodes which are localized in the first step also start acting as anchors, thus improving the accuracy.

All of the above works on localization for underwater wireless networks are based on acoustic waves. Although acoustic waves in underwater can travel for long distances but they suffer from low data rate. Therefore, recently, UOWCs has emerged as a promising technology [2]. UOWC has the advantages of higher data rate, low latency, energy efficiency, and low cost. Therefore, UOWC is considered as a promising technology to develop O-IoUT. Besides the above advantages, it is important to find the location of smart objects in O-IoUT due to its numerous applications, such as data tagging, assisted navigation, and exploring the underwater environment.

Currently, localization for O-IoUT is one of the critical research areas, and various efforts are made to develop accurate localization algorithms. Based on the implementations, these algorithms can be broadly classified into distributed and centralized. In distributed algorithms, all the smart objects collect the ranging information from the anchors and localize itself while in centralized algorithms, all the smart

objects in the networks are localized by the central node. Akhoundi *et al.* [7] proposed a ToA- and RSS-based distributed localization method for O-IoUT. Optical base stations (OBSs) were used as anchors, which transmit the optical signals, and the smart objects were able to collect the optical signals from multiple OBSs. Each of the OBSs consisted of 60 light emitted diodes (LEDs) transmitters forming an underwater optical code division multiple access (OCDMA) network. In the ToA-based approach, it was assumed that all the OBSs are synchronized and the distance was estimated from the time of flight of the optical signal in water. Linear least square solution was used by the sensors to locate their positions based on the optical signals received from various OBSs. In the RSS-based approach, the distance was estimated from the UOWC channel model where the received power is greatly affected by various impairments, such as attenuation, scattering, turbulence, and multipath. Akhoundi *et al.* [7] used Monte-Carlo simulations to estimate the distance from the received optical power. Although the RSS-based approach is easy to implement, and it provides coarse localization. Saeed *et al.* [8] proposed a centralized localization technique for O-IoUT by taking into account the limited connectivity of UOWCs. All of the ranging measurements were collected at the surface node, where the multidimensional (MDS) technique was used to estimate the location of each sensor node. The proposed localization algorithm in [8] was further improved in [10] by using the energy harvested from ambient underwater sources. It was shown in [10] that the energy arriving into the network improves the localization accuracy. Moreover, a low-rank matrix completion strategy was used in [26] to estimate the missing pairwise distances for a centralized RSS-based 3-D localization technique. Nevertheless, a 3-D localization technique for O-IoUT was recently proposed in [11] which accounts for outliers produced in the range measurements. Also, the locations of the anchors were optimized for the whole network in [11] to achieve better localization accuracy. Recently, vector quantization was used in [27] for the localization of smart objects in O-IoUT.

Another challenging problem for 3-D localization of smart objects in O-IoUT networks is the placement of anchors to improve the accuracy. Conventionally, the anchors should be spread uniformly along the perimeter of the network [28]. The literature on the optimization of the anchors' location can be categorized into two major classes. First is the parameter optimization techniques, where the position of the smart objects is estimated such that their location uncertainty is minimized. The uncertainty in the position is characterized by the inverse of the Cramer–Rao lower bound (CRLB), i.e., the Fisher information matrix (FIM). Therefore, these techniques try to maximize the FIM or minimize the CRLB by changing the positions of the anchors along the network [12], [29]–[34]. For instance, Hamdollahzadeh *et al.* [12] used time difference of arrival and frequency difference of arrival ranging methods to optimize the anchor placement for a single target. It was shown in [12] that the combination of uniform angular arrays could be used for the optimal placement of anchors. A similar analysis with the angle-of-arrival-, ToA-, and RSS-based ranging was presented in [30]–[32], respectively, for a single target where it was shown that there is no unique optimal anchors geometry. A closed-form solution of optimal anchor placement for a single target was proposed in [29] where it was concluded that multiple nontrivial local solutions exist. Geometric dilution of the precision-based approach was investigated in [33], to optimize the anchor location for multiple primary users localization in cognitive radio networks. Recently, Rusu and Thompson [34] used the concept of tight frames for the anchor location optimization with the time difference of arrival ranging method. All of these methods try to find the geometry of the anchors, which minimized the CRLB of the network. The second class of anchor optimization techniques is optimal control, which is mainly used for the path planning problems [35], [36]. All of these works consider the optimization of the anchor's location for a single target or the whole network.

However, none of these works consider optimizing the position of anchors for a specific set of valuable sensors. Since in many application scenarios, it is not desirable to optimize the location of anchors for all the smart objects in the network. Therefore, it is more crucial to find the location of valuable sensors more accurately compared to the other smart objects in the network. Hence, in this article, we propose a 3-D accurate localization technique by selecting the set of vital sensors by using spectral clustering and optimizing anchors' location for these sensors.

III. Problem Formulation

In this section, we formulate the problem of 3-D localization for selected smart objects. Consider a 3-D O-IoUT network with N static smart objects which can be underwater sensors using optical waves for communications and M mobile anchor nodes (surface buoy) as shown in Fig. 1. The smart objects consist of sensors/actuators and are static in nature where they are either attached to the seabed or moored. The information from the seabed sensors is collected at the surface buoy in a multihop fashion via the moored smart objects [37]. Here, we consider self-propelled surface buoys that can move on the surface of the water as well as they can dive and rise to surface [24]. If the surface buoys, which are also acting as anchors, are located at the surface only, the localization problem in 3-D cannot be solved regardless of the number of surface buoys deployed. Therefore, for the 3-D localization, we assume that the projection (depth) of each buoy is different such that they are not co-planer [38]. Also, we assume that some of the smart objects (green ones) detects the target/activity and thus has more valuable information. Therefore, accurate localization of these smart objects is more important compared to other smart objects in the network. Every network localization technique necessitates for estimating the smart object-to-smart object and smart objects-to-anchor distances. These distances can be estimated by using various ranging methods, such as time-based, angle-based, and received power-based methods. The time-based localization techniques provide higher localization accuracy; however, they require additional hardware on the underwater resource-limited smart objects. Also, the time-based methods heavily rely on synchronization between the smart objects and the surface buoy.

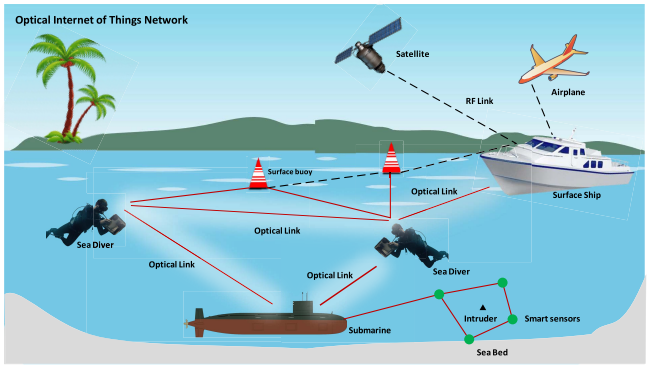

Fig. 1. O-IoUT network.

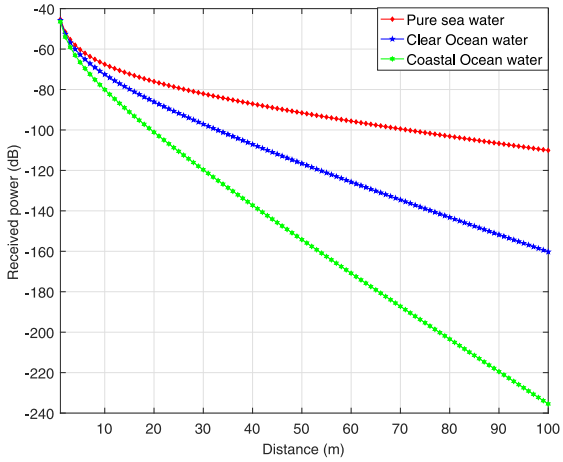

Fig. 2. Received power versus distance for different types of water.

Similarly, the angle-based ranging techniques are more accurate but have high complexity and consume more power [39]. On the other hand, the RSS-based localization techniques have low localization accuracy, but they do not require extra hardware and have low complexity. Hence, the RSS-based methods suit well for the resource-limited O-IoUT networks thanks to their simplicity and cost efficiency. Therefore, in this article, we assume that the single neighborhood noisy distances are estimated by using the RSS-based underwater optical ranging [40].

Since RSS-based ranging depends on the propagation behavior of light in water, therefore, first, we briefly discuss the link budget of a UOWC channel (UOWC). The propagation of light in underwater aquatic medium suffers from scattering and absorption which is characterized by the well-known Haltran's model as follows:

$$E(\lambda) = B(\lambda) + S(\lambda) \tag{1}$$

where λ is the wavelength, and $E(\lambda)$, $B(\lambda)$, and $S(\lambda)$ are the extinction, absorption, and scattering coefficients, respectively. Optical light traveling in the aquatic medium is mainly absorbed by the chlorophyll, hence, $B(\lambda)$ is given as

$$B(\lambda) = B_p(\lambda) + B_c(\lambda) + B_f C_f \exp^{-a_f \lambda} + B_h C_h \exp^{-a_h \lambda} \tag{2}$$

where $B_p(\lambda)$, $B_c(\lambda)$, $B_f = 35.959$ m^2/mg, and $B_h = 18.828$ m^2/mg are the absorption coefficients of pure water, chlorophyll, fulvic acid, and humic acid, respectively. The terms a_f and a_h are constants, whereas C_f and C_h are the concentrations of fulvic acid and humic acid, respectively. The values of C_f and C_h are given in [41] as follows:

$$C_f = 1.74098 C_x \exp^{\left(0.12327 \frac{C_x}{C_y}\right)} \tag{3}$$

and

$$C_h = 0.19334 C_x \exp^{\left(0.12343 \frac{C_x}{C_y}\right)} \tag{4}$$

where $0 \leq C_x \leq 12$ mg/m^2 and $C_y = 1$ mg/m^3. Correspondingly, $S(\lambda) = S_p(\lambda) + S_s(\lambda)C_s + S_l(\lambda)C_l$, where $S_p(\lambda) = 0.005826(400/\lambda)^{4.322}$, $S_s(\lambda) = 1.151302(400/\lambda)^{1.7}$, and $S_l(\lambda) = 0.341074(400/\lambda)^{0.3}$ are the scattering coefficients for pure seawater, small particles, and large particles, respectively. The concentration of small and large particles is represented by $C_s = 0.01739 C_x \exp^{\{0.11631(C_x/C_y)\}}$ and $C_l = C_x \exp^{\{0.03092(C_x/C_y)\}}$, respectively [41]. Based on the value of $E(\lambda)$ for a given aquatic medium, the received power from node i at node j is given in [3] as follows:

$$P_r = P_t \varrho_t \varrho_r \exp^{\left(\frac{-E(\lambda) d_{ij}}{\cos \theta_{ij}}\right)} \frac{A_r \cos \theta_{ij}}{2\pi d_{ij}^2 (1 - \cos \theta_0)} \tag{5}$$

where P_t is the transmit power, d_{ij} and θ_{ij} are the Euclidean distance and trajectory angle between smart objects i and j, ϱ_t and ϱ_r are their optical efficiencies, A_j is the aperture area of the receiver, and θ_0 is the divergence angle. The RSS-based ranges are obtained from (5) as follows:

$$d_{ij} \triangleq f(P_r) = \frac{2}{E(\lambda)} W_0 \left(\frac{e(\lambda)}{2} \sqrt{\frac{P_t \varrho_i \varrho_j A_r \cos \theta_{ij}}{P_r 2\pi (1 - \cos \theta_0)}} \right) \tag{6}$$

where $W_o(\cdot)$ is the real part of Lambert-W function [42]. The above RSS-based ranging model has been experimentally validated in [43] for different wavelengths and various types of water. The model the noise in the ranging measurements, we consider three primary noise sources. The thermal noise of the receiver which follows Gaussian distribution, shot noise which is caused by optical filtering and is also modeled by Gaussian distribution, and intensity noise to model the fluctuation in the intensity of light (Gaussian). The superposition of all these noise sources results in a memory-less additive Gaussian noise, and therefore, the received power can be written as

$$\hat{P}_r = P_r + n_{ij} \tag{7}$$

where n_{ij} represents the noise that is modeled as a zero mean Gaussian random variable $n_{ij} \sim \mathcal{N}(0, \sigma_{ij}^2)$ with variance σ_{ij}^2. The noisy range measurements are obtained from (7) as $\hat{d}_{ij} = f(\hat{P}_{r_{ij}})$. Fig. 2 shows the relationship between the received power and the distance for various water types, such as pure sea water, clear ocean water, and coastal ocean water. The simulation parameters are mainly taken from [44]. Fig. 2 shows that increase in the distance and turbidity of the water reduces the power received.

To find the multihop pairwise distances, we model the network as a connected graph $G(V, E)$, where V are the vertices and E are the edges of the graph. Vertices V refer

to the unknown location of the smart objects and edges E are the estimated distances. Once the network is modeled as a connected graph, the missing pairwise distances between faraway smart objects are estimated by using a matrix completion method. Additionally, it is crucial for the accuracy of any network localization technique to optimize the location of anchors. In previous research works, the problem of optimizing anchor locations for a single target node or all smart objects have been investigated. In this article, first, we find the coarse 3-D location of each smart object in the network and then optimize the anchor locations for the specific set of smart objects. Optimizing the anchor locations for a set of significant smart objects is more interesting and challenging. Therefore, the problem of accurate 3-D localization for a set of smart objects $S \subset N$ is straightforward, i.e., for a given O-IoUT setup with estimated pairwise distances $\hat{\mathbf{D}} = \{\hat{d}_{ij}\}_{i\neq j}^{N+M}$, optimize the location of anchors for S number of smart objects to estimate their location $\hat{\mathbf{L}} = \{\hat{x}_i, \hat{y}_i, \hat{z}_i\}_{i=1}^{S}$ with improved accuracy.

IV. Proposed Technique

In this section, we propose an accurate localization technique where the location of anchors is optimized for a set of smart objects instead of all the objects. The proposed 3-D localization technique consists of the following four steps: 1) construction of the pairwise distance estimation matrix $\hat{\mathbf{D}}$; 2) selection of the set of smart objects S; 3) partitioning of $\hat{\mathbf{D}}$ into a local pairwise distance estimation matrix $\hat{\mathbf{D}}_l$; and 4) optimization of the anchor locations to improve the localization accuracy.

A. Construction of Matrix $\hat{\boldsymbol{D}}$

In this step, the pairwise distances are estimated between all the smart objects in the network. The estimated distance between any two neighbor smart objects i and j are calculated in the previous section and given as

$$\hat{d}_{ij} = d_{ij} + \eta_{ij} \tag{8}$$

where $d_{ij} = \sqrt{(x_i - x_j)^2 + (y_i - y_j)^2 + (z_i - z_j)^2}$ and η_{ij} is the ranging error. The ranging error is modeled as zero mean Gaussian random variable with variance σ_{ij}^2. All of the single neighborhood measured distances are shared with the surface station in a multihop fashion. The surface station create a network graph $G(V, E)$ by collecting all of the single neighborhood noisy distances. The edges of the graph represent the noisy distances, and can be written in the matrix form as

$$\hat{\mathbf{D}} = \begin{bmatrix} 0 & \hat{d}_{12} & \dots & \hat{d}_{1N} \\ \hat{d}_{21} & 0 & \dots & \hat{d}_{2N} \\ \vdots & \vdots & \ddots & \vdots \\ \hat{d}_{N1} & \hat{d}_{N2} & \dots & 0 \end{bmatrix}. \tag{9}$$

However, many of the pairwise noisy distances are missing and only a set of them are available. Therefore, a matrix completion strategy is required to estimate the missing distances [45]. Here, we consider the low-rank matrix completion technique to estimate the missing pairwise distances in matrix $\hat{\mathbf{D}}$ [26]. Once the missing pairwise distances are estimated, matrix $\hat{\mathbf{D}}$ is completed.

B. Selection of Smart Objects

Cluster-based schemes are most widely applied to localize a specific target or activity in cyber-physical systems, which improves the scalability of the network and reduces the communication overhead [46]. Besides, the smart objects which participate in the target detection or the activity are kept active while the rest of the smart objects are left inactive to consume the resources efficiently. The cluster-based schemes should be able to decide on which smart object to be included or excluded from the cluster. This selection of smart objects can be based on multiple criteria, such as quality of the sensed data, distance to the target/activity region, and residual energy. In this article, we consider the usefulness of the information and proximity to the target/activity region as a selection criterion for smart objects. For instance, we assume that the sensed information and location of smart objects which detect the target or in the vicinity of the activity are more critical compared to the other smart objects. Hence, it is required to select those set of smart objects which have more valuable information and are near to the target/activity region. Therefore, we use a graph partitioning technique to split the network into subnetworks [47]. As the network graph is represented by $G(V, E)$, where $V = \{1, 2, \dots, N\}$ and E are the edges. Partitioning of $G(V, E)$ means to get k number of disjoint connected graphs, i.e., $V = V_1 \cup V_2 \cup, \dots, \cup V_k$. Graph partitioning is one of the most widely used methods for data analysis where its applications lie in statistics, biology, computer science, and psychology. The graph partitioning techniques help in identifying the behavior of the data where similar data is grouped into a single partition.

The graph partitioning technique consists of two phases, i.e., partition the graph into two graphs and then repeat the same process until reaching k number of subsets. To partition $G(V, E)$, first, we define the adjacency matrix $\mathbf{A}(G)$ of the graph such that its elements are given as

$$a_{ij} = \begin{cases} 1, & (i,j) \in E \\ 0, & (i,j) \notin E. \end{cases} \tag{10}$$

Also, we define the degree matrix $\mathbf{Q}$, which represents the degree of connectivity of each node. Based on $\mathbf{A}(G)$ and $\mathbf{Q}$, the Laplacian matrix of $\hat{\mathbf{D}}$ is calculated as $\mathbf{L} = \mathbf{Q} - \hat{\mathbf{D}}$. Subsequently, eigenvalues $\lambda_1 \leq \lambda_2 \leq \cdots \leq \lambda_N$ and eigenvectors $\mathbf{w}_1, \mathbf{w}_2, \dots, \mathbf{w}_N$ of $\mathbf{L}$ are calculated. Graph $G(V, E)$ is partitioned based on the second eigenvector $\mathbf{w}_2$ (also known as Fiedler vector) of the Laplacian matrix [47], [48]. To further elaborate, we consider a connected graph Y, as shown in Fig. 3(a). The Laplacian matrix $\mathbf{L}(Y)$ for graph Y is given as

$$\mathbf{L}(Y) = \begin{bmatrix} 3 & -1 & 0 & 0 & 0 & 0 & -1 & -1 & 0 & 0 \\ -1 & 2 & -1 & 0 & 0 & 0 & 0 & 0 & 0 & 0 \\ 0 & -1 & 2 & -1 & 0 & 0 & 0 & 0 & 0 & 0 \\ 0 & 0 & -1 & 2 & -1 & 0 & 0 & 0 & 0 & 0 \\ 0 & 0 & 0 & -1 & 2 & -1 & 0 & 0 & 0 & 0 \\ 0 & 0 & 0 & 0 & -1 & 2 & -1 & 0 & 0 & 0 \\ -1 & 0 & 0 & 0 & 0 & -1 & 2 & 0 & 0 & 0 \\ -1 & 0 & 0 & 0 & 0 & 0 & 0 & 3 & -1 & -1 \\ 0 & 0 & 0 & 0 & 0 & 0 & 0 & -1 & 2 & -1 \\ 0 & 0 & 0 & 0 & 0 & 0 & 0 & -1 & -1 & 2 \end{bmatrix}. \tag{11}$$

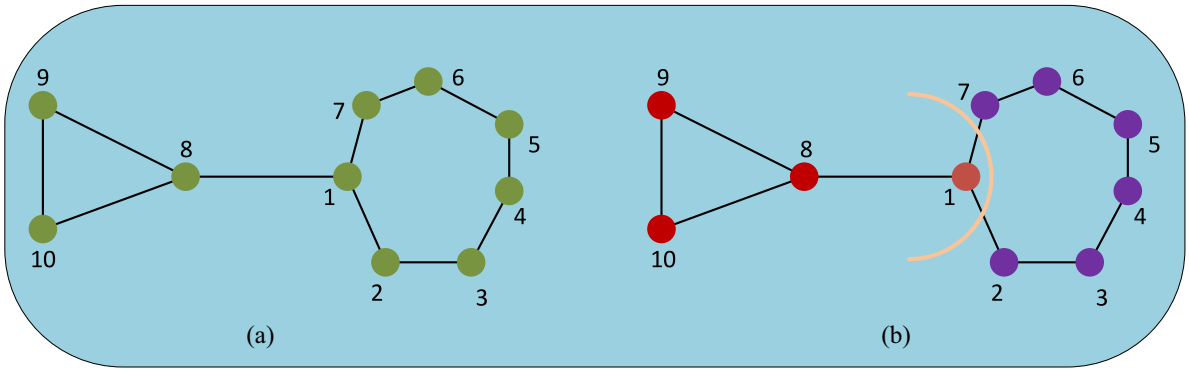

Fig. 3. Spectral clustering of a graph. (a) Graph Y with associated vertices and links. (b) Graph Y after partitioning into two subgraphs.

Algorithm 1: Graph Partitioning Algorithm

Input: Graph $G(V, E)$;
Output: Set of partitioned graphs, $V_1, V_2, \ldots, V_k$;
Compute the Laplacian matrix of $\hat{\mathbf{D}}$;
Compute the Fiedler vector of $\mathbf{L}$;
for $i = 1 : N$ **do**
  if *Fiedler vector*$_i < 0$ **then**
    Node i belongs to partition V_1;
    i + +;
    else if *Fiedler vector*$_i > 0$ **then**
      Node i belongs to partition V_2;
    end
    i + +;
  end
  Continue until k number of partitions are completed;
end

The corresponding Fiedler vector $\mathbf{w}_Y$ is given as

$$\mathbf{w}_Y = [0.0521, -0.1147, -0.2543, -0.3335, -0.3335 - 0.2543, -0.1147, 0.3734, 0.4897, 0.4897]^T. \quad (12)$$

Based on the values of $\mathbf{w}_Y$, the vertices which correspond to the negative values are placed in one subgraph while the vertices corresponding to the positive values of $\mathbf{w}_Y$ are placed into the other subgraph. This partitioning is shown in Fig. 3(b). This partition may not look perfect since it does not reduce the number of edges at the partition point and removing edge (1, 8) could be a better choice. Similarly, if an equal number of vertices were required to be placed in each subgraph then edge (6, 7) should be the cut point. This way each subgraph will have five vertices. However, the Fiedler spectral partitioning tries to balance both the number of vertices in each subgraph and having less number of edges at the cut point. Although the Fiedler spectral partitioning method is not flawless, it does not require the coordinates of the vertices thus making it more suitable for the clustering of O-IoUT network. Details of the graph partitioning algorithm are given in Algorithm 1.

C. Local Pairwise Distance Estimation Matrix

Once a set of S smart objects is selected among N number of smart objects by using the graph partitioning technique. A local pairwise distance estimation matrix $\hat{\mathbf{D}}_l$ is constructed from $\hat{\mathbf{D}}$. The size of $\hat{\mathbf{D}}_l$ is $S \times S$ which is smaller than the size of $\hat{\mathbf{D}}$. The MDS technique is used to get the 3-D map of the network where the MDS technique takes $\hat{\mathbf{D}}_l$ as an input and generates the 3-D map. The MDS method tries to minimize the cost function given as [49]

$$f(\hat{d}_{ij}|\mathbf{L}) = \sum_{j>i}^{S} \left(\frac{\hat{d}_{ij} - d_{ij}(\mathbf{L})}{\hat{d}_{ij}} \right)^2 \quad (13)$$

where $\mathbf{L} = \{x_i, y_i, z_i\}_{i=1}^{S}$. The main objective of the MDS technique is to find matrix $\mathbf{L}$ such that $\hat{d}_{ij}$ matches d_{ij} as close as possible. The closed-form solution of (13) is obtained by first double centering matrix $\hat{\mathbf{D}}_l$, i.e., $\mathbf{B} = -0.5\mathbf{C}\hat{\mathbf{D}}_l\mathbf{C}$ where $\mathbf{C} = \mathbf{I}_S - ([\mathbf{1}_S\mathbf{1}_S^T]/S)$ is the centering matrix. $\mathbf{I}_S$ is an $S \times S$ identity matrix and $\mathbf{1}_S$ is the vector of 1s with size S. Taking the eigenvalue decomposition of matrix $\mathbf{B}$ yields its corresponding eigenvalues $\boldsymbol{\lambda}$ and eigenvectors $\mathbf{e}$ where the 3-D map is obtained from the three largest eigenvalues of $\boldsymbol{\lambda}$ and corresponding three eigenvectors in $\mathbf{e}$, i.e., $\hat{\mathbf{L}} = \boldsymbol{\lambda}_3\sqrt{\mathbf{e}_3}$, where the size of $\boldsymbol{\lambda}_3$ and $\mathbf{e}_3$ is 3×3 and $3 \times S$, respectively. The relative 3-D map can be a transformed to a global 3-D map by using any linear transformation method, i.e., $\tilde{\mathbf{L}} = \zeta(\hat{\mathbf{L}})\boldsymbol{r} + \boldsymbol{t}$, where ζ, $\boldsymbol{r}$, and $\boldsymbol{t}$ represent the scaling, rotation, and translation elements, respectively.

D. Optimization of Anchor Positions for Selected Set of Smart Objects

The final step of the proposed technique is to optimize the anchor locations for the selected set of smart objects to improve their localization accuracy. As in Section IV-A, the pairwise noisy distances are calculated for the selected set of smart objects, now the location of anchors is optimized to improve their localization accuracy. The distance estimated between a smart object in S and the jth anchor node is $\hat{d}_j = d_j + n_j$, for $j = 1, 2, \ldots, M$, where $d_j = \sqrt{(x - x_j)^2 + (y - y_j)^2 + (z - z_j)^2}$ and n_j is the ranging error. As n_j is modeled as Gaussian random variable with variance σ_j^2 then error variance of 3-D location estimation is bounded by the CRLB, i.e., $\mathcal{B}(\tilde{\boldsymbol{l}}) = \boldsymbol{F}^{-1}(\boldsymbol{l})_{i,i}$ for the ith parameter [50].

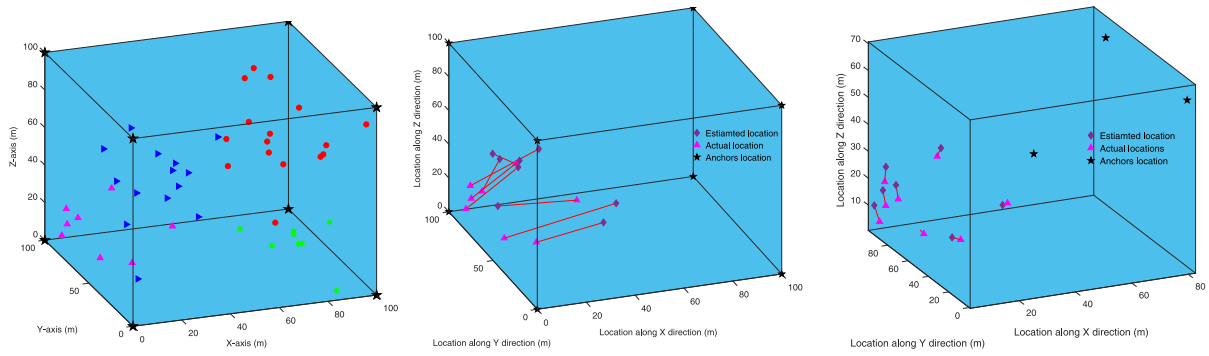

(a) (b) (c)

Fig. 4. (a) O-IoUT setup (50 smart objects). (b) Selected set of smart objects localization without optimization of anchors' location. (c) Selected set of smart objects localization with optimization of anchors' location.

$\boldsymbol{F}(\boldsymbol{l})$ represents the FIM with elements given as

$$\boldsymbol{F}(\boldsymbol{l})_{i,j} = -E\left(\frac{\partial^2 \log f(\hat{\boldsymbol{d}}|\boldsymbol{l})}{\partial \boldsymbol{l}_i \partial \boldsymbol{l}_j}\right), \qquad i,j = 1,2,3 \tag{14}$$

where E is the expectation operator and $\hat{\boldsymbol{d}} = \{\hat{d}_1, \hat{d}_2, \ldots, \hat{d}_M\}$. The probability density function $f(\hat{\boldsymbol{d}}|\boldsymbol{l})$ for the noisy range measurements is defined as

$$f\left(\hat{\boldsymbol{d}}|\boldsymbol{l}\right) = \frac{1}{\sqrt{(2\pi)^M \prod_{j=1}^{M} \sigma_j}} \exp\left(-\sum_{j=1}^{M} \frac{1}{2\sigma_j^2}\left(\hat{d}_j - d_j\right)^2\right). \tag{15}$$

The submatrices of $\boldsymbol{F}(\boldsymbol{l})_{i,j}$ are derived from (14) and given as

$$\boldsymbol{F}(\boldsymbol{l})_{i=1,j=1} = \sum_{k=1}^{M}\left(\frac{(x-x_k)}{\sigma_k d_k}\right)^2 \tag{16}$$

$$\boldsymbol{F}(\boldsymbol{l})_{i=1,j=2} = \boldsymbol{F}(\boldsymbol{l})_{i=2,j=1} = \sum_{k=1}^{M}\left(\frac{(x-x_k)(y-y_k)}{(\sigma_k d_k)^2}\right) \tag{17}$$

$$\boldsymbol{F}(\boldsymbol{l})_{i=1,j=3} = \boldsymbol{F}(\boldsymbol{l})_{i=3,j=1} = \sum_{k=1}^{M}\left(\frac{(x-x_k)(z-z_k)}{(\sigma_k d_k)^2}\right) \tag{18}$$

$$\boldsymbol{F}(\boldsymbol{l})_{i=2,j=2} = \sum_{k=1}^{M}\left(\frac{(y-y_k)}{\sigma_k d_k}\right)^2 \tag{19}$$

$$\boldsymbol{F}(\boldsymbol{l})_{i=2,j=3} = \boldsymbol{F}(\boldsymbol{l})_{i=3,j=2} = \sum_{k=1}^{M}\left(\frac{(y-y_k)(z-z_k)}{(\sigma_k d_k)^2}\right) \tag{20}$$

$$\boldsymbol{F}(\boldsymbol{l})_{i=3,j=3} = \sum_{k=1}^{M}\left(\frac{(z-z_k)}{(\sigma_k d_k)}\right)^2. \tag{21}$$

Finally, the CRLB for the 3-D location estimation is

$$\mathcal{B}(\tilde{x}) = \frac{1}{\det(\boldsymbol{F}(\boldsymbol{l}))}\left(\boldsymbol{F}(\boldsymbol{l})_{i=2,j=2}\boldsymbol{F}(\boldsymbol{l})_{i=3,j=3} - \boldsymbol{F}(\boldsymbol{l})^2_{i=2,j=3}\right) \tag{22}$$

$$\mathcal{B}(\tilde{y}) = \frac{1}{\det(\boldsymbol{F}(\boldsymbol{l}))}\left(\boldsymbol{F}(\boldsymbol{l})_{i=1,j=1}\boldsymbol{F}(\boldsymbol{l})_{i=3,j=3} - \boldsymbol{F}(\boldsymbol{l})^2_{i=1,j=3}\right) \tag{23}$$

$$\mathcal{B}(\tilde{z}) = \frac{1}{\det(\boldsymbol{F}(\boldsymbol{l}))}\left(\boldsymbol{F}(\boldsymbol{l})_{i=1,j=1}\boldsymbol{F}(\boldsymbol{l})_{i=2,j=2} - \boldsymbol{F}(\boldsymbol{l})^2_{i=1,j=2}\right). \tag{24}$$

Based on the CRLB analysis, the optimal location estimation of anchors is formulated as a determinant (D)-optimality criteria, i.e., $\check{\mathbf{L}}_a = \text{argmax}_{\check{\mathbf{L}}_a} \sum_{i=1}^{S} |\boldsymbol{F}_i|$, where $\check{\mathbf{L}}_a \in \mathbb{R}^{M\times 3}$ are the optimal location of anchors, $i = 1,2,\ldots,S$ is the set of selected smart objects, and $|\cdot|$ is the notation for the determinant. Intuitively, the above maximization problem can be solved by minimizing the CRLB, i.e., $\check{\mathbf{L}}_a = \text{argmin}_{\check{\mathbf{L}}_a} \sum_{i=1}^{S} \mathcal{B}(\tilde{\boldsymbol{l}}_i)$. The above optimization problem is non-convex and therefore, its approximate solution is obtained by using an iterative gradient method, i.e., $\mathbf{L}_a(t+1) = \mathbf{L}_a(t) - \mu^t \nabla_i(\mathcal{B}(\tilde{\boldsymbol{l}}_i(t))$, where μ^t is the step size, t represents the iteration number, and symbol $\nabla_i(\cdot)$ mean the gradient. The locations of anchors are updated if $\mathcal{B}(\tilde{\boldsymbol{l}}_i(t+1)) < \mathcal{B}(\tilde{\boldsymbol{l}}_i(t))$, however, when $\mathcal{B}(\tilde{\boldsymbol{l}}_i(t+1)) > \mathcal{B}(\tilde{\boldsymbol{l}}_i(t))$ the algorithm stops because the CRLB is not reduced, and therefore, $\mathbf{L}_a(t) = \check{\mathbf{L}}_a$.

Unlike, the acoustic-based underwater networks, optical waves in O-IoUT are a promising transmission carrier for enabling ultrareliable low latency communications, due to their ability to achieve broadband links with high data rate (Gb/s) and low latency [51]. For instance, the average propagation speed of acoustic waves in water is 1500 m/s, which has profound implications on synchronization and localization in an underwater environment. Therefore, O-IoUT provides low-latency and high-bandwidth solutions to its counterpart acoustic technology.

V. Simulation Results

In this section, the results of the proposed localization technique are presented. An O-IoUT network with 50 smart objects randomly distributed in a cubic region of 100 m^3 is considered. The number of anchors is kept to 8 and the maximum transmission range is considered as 100 m. We have considered clean ocean water for these simulations with the scattering coefficient of $S(\lambda) = 0.037$ and absorption coefficient of $B(\lambda) = 0.114$. Fig. 4(a) shows a realization of the simulation

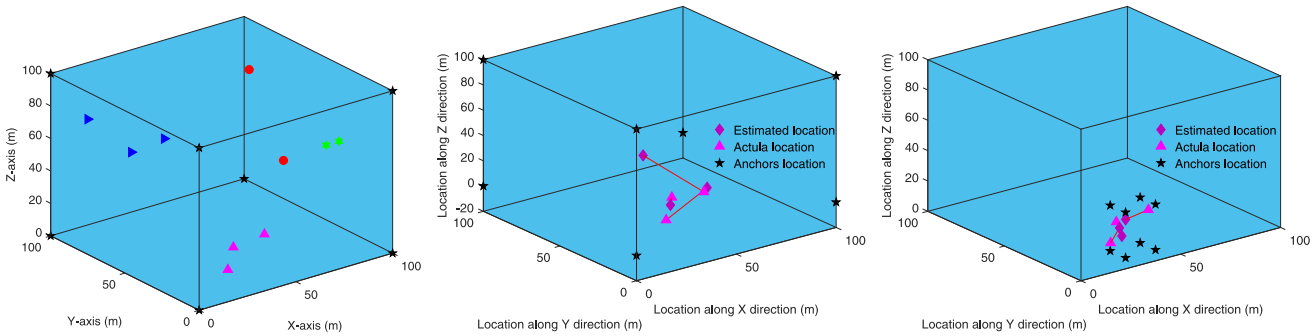

Fig. 5. (a) O-IoUT setup (ten smart objects). (b) Selected set of smart objects localization without optimization of anchors' location. (c) Selected set of smart objects localization with optimization of anchors' location.

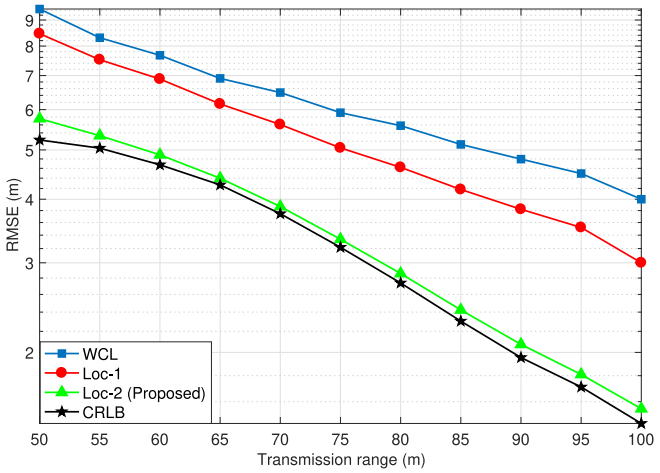

Fig. 6. RMSE versus transmission range.

setup where the smart objects are partitioned into four different clusters. We have assumed that the set of smart objects ($S = 8$) with the data from the pink color smart objects is more valuable and therefore it is required to improve their localization accuracy. The results are obtained as an average of over 10^3 different realizations and compared to [11], [52], and the CRLB.

Fig. 4(b) and (c) shows the localization accuracy of [11] (Loc-1) and the proposed method (Loc-2) for a single realization, respectively, where it is clear that the optimization of the anchor's location for the selected set of smart objects improves the localization accuracy. Moreover, we have also evaluated the performance of the proposed scheme in a sparse network with ten smart objects randomly distributed in 100 m^3 region, as shown in Fig. 5(a). Three smart objects [pink color triangles in Fig. 5(a)] among the total ten objects are selected as valuable objects by the Fiedler partitioning algorithm. Fig. 5(b) and (c) shows that in case of even sparsely populated nodes, the proposed scheme has better localization accuracy due to anchors location optimization.

A. Impact of Transmission Range and Power

As the transmission range is an important parameter for the network localization methods, therefore, root-mean-square-error (RMSE) is evaluated with respect to the transmission range of smart objects in Fig. 6. Fig. 6 shows that the RMSE performance of the proposed method for the selected set of smart objects is better than Loc-1 and weighted centroid localization [52] due to the optimal placement of anchors for these smart objects. Fig. 6 also suggests that increasing the transmission range improves the localization accuracy of both techniques due to the increase in connectivity of the network. As the transmission range increases more smart objects are directly connected to each other which reduces the multihop distance estimation error. Note that the transmission range is increased by playing with the transmission power of the smart objects where high transmission power leads to a more extended range. By increasing the transmission range, the localization accuracy improves since more smart objects are directly connected, reducing the shortest path estimation error.

B. Impact of Ranging Error

Undoubtedly, the distance estimation is affected by the ranging error. Therefore, we have assumed in Section II that the ranging error η_{ij} between any two smart objects i and j are modeled as a zero-mean Gaussian random variable with variance σ_{ij}^2. The performance of the proposed technique is examined with respect to the variable σ_{ij}^2, i.e., $\sigma_{ij}^2 = 0 - 1$ m. Here, we considered 50 optical smart objects randomly placed in a cubic region of 100 m^3 with the maximum transmission range of 100 m and the results are averaged over 10^3 different realizations. In Fig. 7, we show that the RMSE performance is affected by the ranging error noise variance. Fig. 7 shows that Loc-2 has better RMSE performance as compared to Loc-1 in [11]. Moreover, Fig. 7 also presents that an increase in the noise variance increases the RMSE for all the techniques. Moreover, since the underwater channel is highly dynamic, the RMSE concerning multiple RSS measurements is investigated in Fig. 8. We have simulated two different O-IoUT networks with 50 and 100 smart objects distributed randomly in a cubic region of $100 \times 100 \times 100$ m^3, respectively. Here, we keep the transmission range of smart objects equal to 100 m. Fig. 8 shows that the localization accuracy improves with the increase in the number of measurements up to a particular

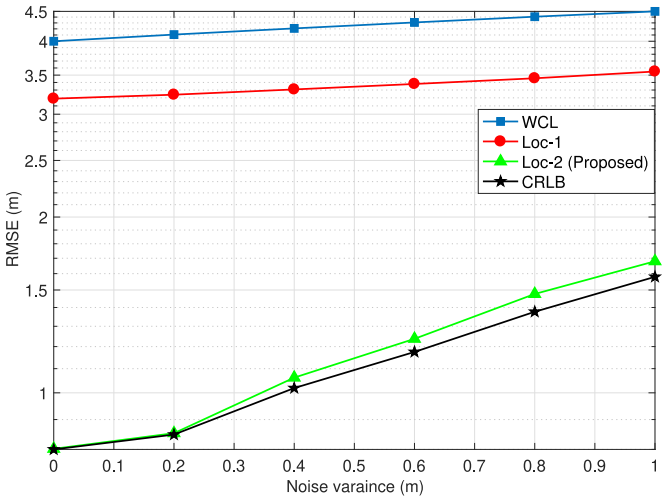

Fig. 7. RMSE versus noise variance.

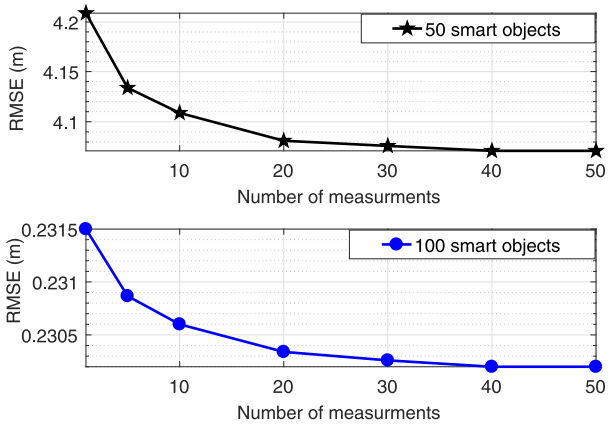

Fig. 8. RMSE versus number of RSS measurements.

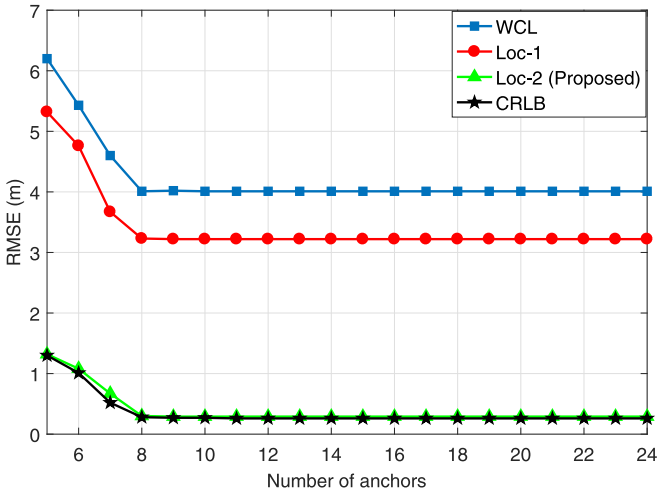

Fig. 9. RMSE versus anchors.

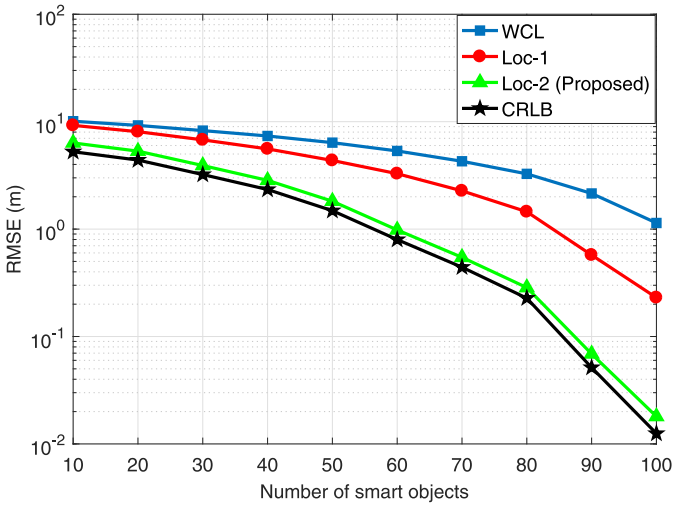

Fig. 10. RMSE versus number of smart objects.

value, i.e., 20, after which the RMSE is saturated and does not improve further.

C. Impact of Number of Anchors

Anchors play a vital role in localization algorithms, and it is a fact that with increasing the number of anchors, the accuracy becomes better. Therefore, we show this effect in Fig. 9, where the RMSE performance improves with an increase in the number of anchors up to a certain number, i.e., 8, after which the network gets saturated and further increases in the number of anchors do not improve the accuracy. Note that for these results, we considered the same simulation setup consisting of 50 smart objects randomly distributed in a cubic region of 100 m^3 and the results are obtained over 10^3 different realizations.

D. Impact of Node Density

The network localization techniques are greatly affected by the density of the network. The accuracy of the proposed scheme primarily depends on the density of the smart objects for a given network area. To see the connection between the localization accuracy and node density, we have evaluated the performance of the proposed scheme with respect to the different density of the network. Initially, we started with a sparse network of ten smart objects only in a cubic region of 100 m^3 and then increase the density to 100 smart objects. Fig. 10 shows that increasing the number of smart objects improves the RMSE. This is due to higher connectivity in the network where each smart object is having more neighbors (reducing the shortest path error). Moreover, Fig. 10 also tells that the minimum average number of smart objects required for a connected network is 10. Hence, when the number of smart objects is below 10, it leads to an unconnected network where the smart objects cannot be localized.

VI. Conclusion

The optimization of the anchors' location to improve the localization accuracy of smart objects in a network has been studied well in the past. However, in a number of applications, the data collected from some smart objects are more valuable than others and, hence, the smart objects whose data is more valuable require accurate localization. Therefore, in this article, first, we have partitioned the network into a set of multiple

small networks to select the valuable smart objects by using a graph partitioning technique. Then, we have optimized the anchor nodes' location to improve the localization accuracy of the selected set. The numerical results validate the accuracy and robustness of the proposed technique.

REFERENCES

[1] E.-C. Liou, C.-C. Kao, C.-H. Chang, Y.-S. Lin, and C.-J. Huang, "Internet of underwater things: Challenges and routing protocols," in *Proc. IEEE Int. Conf. Appl. Sys. Invention (ICASI)*, Apr. 2018, pp. 1171–1174.

[2] N. Saeed, A. Celik, T. Y. Al-Naffouri, and M.-S. Alouini, "Underwater optical wireless communications, networking, and localization: A survey," *Ad Hoc Netw.*, vol. 94, pp. 1–35, Nov. 2019. [Online]. Available: https://www.sciencedirect.com/science/article/pii/S1570870518309776

[3] L. K. Gkoura *et al.*, "Underwater optical wireless communication systems: A concise review," in *Turbulence Modelling Approaches—Current State, Development Prospects, Applications*. Rijeka, Croatia: InTech, 2017.

[4] A. Celik, N. Saeed, T. Y. Al-Naffouri, and M.-S. Alouini, "Modeling and performance analysis of multihop underwater optical wireless sensor networks," in *Proc. IEEE Wireless Commun. Netw. Conf. (WCNC)*, Barcelona, Spain, Apr. 2018, pp. 1–6.

[5] I. F. Akyildiz, D. Pompili, and T. Melodia, "Underwater acoustic sensor networks: Research challenges," *Ad Hoc Netw.*, vol. 3, no. 3, pp. 257–279, May 2005.

[6] M. Erol-Kantarci, H. T. Mouftah, and S. Oktug, "A survey of architectures and localization techniques for underwater acoustic sensor networks," *IEEE Commun. Surveys Tuts.*, vol. 13, no. 3, pp. 487–502, 3rd Quart., 2011.

[7] F. Akhoundi, A. Minoofar, and J. A. Salehi, "Underwater positioning system based on cellular underwater wireless optical CDMA networks," in *Proc. Wireless Opt. Commun. Conf. (WOCC)*, Newark, NJ, USA, Apr. 2017, pp. 1–3.

[8] N. Saeed, A. Celik, T. Y. Al-Naffouri, and M.-S. Alouini, "Underwater optical sensor networks localization with limited connectivity," in *Proc. IEEE Int. Conf. Acoust. Speech Signal Process. (ICASSP)*, Calgary, AB, Canada, Apr. 2018, pp. 1–5.

[9] N. Saeed, A. Celik, M.-S. Alouini, and T. Y. Al-Naffouri, "Performance analysis of connectivity and localization in multi-hop underwater optical wireless sensor networks," *IEEE Trans. Mobile Comput.*, vol. 18, no. 11, pp. 2604–2615, Nov. 2019. [Online]. Available: https://ieeexplore.ieee.org/abstract/document/8515089

[10] N. Saeed, A. Celik, T. Y. Al-Naffouri, and M.-S. Alouini, "Localization of energy harvesting empowered underwater optical wireless sensor networks," *IEEE Trans. Wireless Commun.*, vol. 18, no. 5, pp. 2652–2663, May 2019.

[11] N. Saeed, T. Y. Al-Naffouri, and M.-S. Alouini, "Outlier detection and optimal anchor placement for 3-D underwater optical wireless sensor network localization," *IEEE Trans. Commun.*, vol. 67, no. 1, pp. 611–622, Jan. 2019.

[12] M. Hamdollahzadeh, S. Adelipour, and F. Behnia, "Optimal sensor configuration for two dimensional source localization based on TDOA/FDOA measurements," in *Proc. 17th Int. Radar Symp. (IRS)*, May 2016, pp. 1–6.

[13] K. M. Mridula and P. M. Ameer, "Localization under anchor node uncertainty for underwater acoustic sensor networks," *Int. J. Commun. Syst.*, vol. 31, no. 2, pp. 1–14, 2018.

[14] J. Perez-Ramirez, D. K. Borah, and D. G. Voelz, "Optimal 3-D landmark placement for vehicle localization using heterogeneous sensors," *IEEE Trans. Veh. Technol.*, vol. 62, no. 7, pp. 2987–2999, Sep. 2013.

[15] A. Nanda, P. Nanda, X. He, D. Puthal, and A. Jamdagni, "A novel hybrid authentication model for geo location oriented routing in dynamic wireless mesh networks," in *Proc. Int. Conf. Syst. Sci.*, 2018, pp. 5532–5541.

[16] R. C. Shit, S. Sharma, D. Puthal, and S. S. Tripathi, "Probabilistic RSS fingerprinting for localization in smart platforms," in *Proc. Int. Conf. Inf. Technol. (ICIT)*, Dec. 2018, pp. 254–259.

[17] R. C. Shit *et al.*, "Ubiquitous localization (UbiLoc): A survey and taxonomy on device free localization for smart world," *IEEE Commun. Surveys Tuts.*, to be published.

[18] R. C. Shit, S. Sharma, D. Puthal, and A. Y. Zomaya, "Location of Things (LoT): A review and taxonomy of sensors localization in IoT infrastructure," *IEEE Commun. Surveys Tuts.*, vol. 20, no. 3, pp. 2028–2061, 3rd Quart., 2018.

[19] M. Erol-Kantarci, H. T. Mouftah, and S. Oktug, "A survey of architectures and localization techniques for underwater acoustic sensor networks," *IEEE Commun. Surveys Tuts.*, vol. 13, no. 3, pp. 487–502, 3rd Quart., 2011.

[20] Y. Zhou, B.-J. Gu, K. Chen, J.-B. Chen, and H.-B. Guan, "An range-free localization scheme for large scale underwater wireless sensor networks," *J. Shanghai Jiaotong Univ. (Sci.)*, vol. 14, no. 5, pp. 562–572, Oct. 2009.

[21] D. Mirza and C. Schurgers, "Collaborative localization for fleets of underwater drifters," in *Proc. OCEANS Conf.*, Vancouver, BC, Canada, Sep. 2007, pp. 1–6.

[22] M. Erol-Kantarci, L. F. M. Vieira, and M. Gerla, "AUV-aided localization for underwater sensor networks," in *Proc. Int. Conf. Wireless Algorithms Syst. Appl. (WASA)*, Chicago, IL, USA, Aug. 2007, pp. 44–54.

[23] H. Luo, Z. Guo, W. Dong, F. Hong, and Y. Zhao, "LDB: Localization with directional beacons for sparse 3D underwater acoustic sensor networks," *J. Netw.*, vol. 5, no. 1, pp. 28–38, 2010.

[24] M. Erol-Kantarci, L. F. M. Vieira, and M. Gerla, "Localization with Dive'N'Rise (DNR) beacons for underwater acoustic sensor networks," in *Proc. 2nd Workshop Underwater Netw. (WuWNet)*, Montreal, QC, Canada, 2007, pp. 97–100.

[25] M. Erol-Kantarci, L. F. M. Vieira, A. Caruso, F. Paparella, M. Gerla, and S. Oktug, "Multi stage underwater sensor localization using mobile beacons," in *Proc. 2nd Int. Conf. Sensor Technol. Appl. (Sensorcomm)*, Aug. 2008, pp. 710–714.

[26] N. Saeed, A. Celik, T. Y. Al-Naffouri, and M.-S. Alouini, "Robust 3D localization of underwater optical wireless sensor networks via low rank matrix completion," in *Proc. IEEE Int. Workshop Signal Process. Adv. Wireless Commun. (SPAWC)*, Jun. 2018, pp. 1–5.

[27] Z. Yan, A. Mukherjee, L. Yang, S. Routray, and G. Palai, "Energy-efficient node positioning in optical wireless sensor networks," *Optik*, vol. 178, pp. 461–466, Feb. 2019.

[28] J. N. Ash and R. L. Moses, "On optimal anchor node placement in sensor localization by optimization of subspace principal angles," in *Proc. IEEE Int. Conf. Acoust. Speech Signal Process. (ICASSP)*, Las Vegas, NV, USA, Mar. 2008, pp. 2289–2292.

[29] H. Zhang, "Two-dimensional optimal sensor placement," *IEEE Trans. Syst., Man, Cybern.*, vol. 25, no. 5, pp. 781–792, May 1995.

[30] A. N. Bishop, B. Fidan, B. D. O. Anderson, K. Dogancay, and P. N. Pathirana, "Optimality analysis of sensor-target geometries in passive localization: Part 1—Bearing-only localization," in *Proc. 3rd Int. Conf. Intell. Sensors Sensor Netw. Inf.*, Dec. 2007, pp. 7–12.

[31] A. N. Bishop, B. Fidan, B. D. O. Anderson, P. N. Pathirana, and K. Dogancay, "Optimality analysis of sensor-target geometries in passive localization: Part 2—Time-of-arrival based localization," in *Proc. 3rd Int. Conf. Intell. Sensors Sensor Netw. Inf.*, Dec. 2007, pp. 13–18.

[32] A. N. Bishop and P. Jensfelt, "An optimality analysis of sensor-target geometries for signal strength based localization," in *Proc. Int. Conf. Intell. Sensors Sensor Netw. Inf. Process.*, Melbourne, VIC, Australia, Dec. 2009, pp. 127–132.

[33] N. Saeed and H. Nam, "Energy efficient localization algorithm with improved accuracy in cognitive radio networks," *IEEE Commun. Lett.*, vol. 21, no. 9, pp. 2017–2020, Sep. 2017.

[34] C. Rusu and J. Thompson, "On the use of tight frames for optimal sensor placement in time-difference of arrival localization," in *Proc. 25th Eur. Signal Process. Conf. (EUSIPCO)*, Aug. 2017, pp. 1415–1419.

[35] X. Xu, "Impulsive control in continuous and discrete-continuous systems," *IEEE Trans. Autom. Control*, vol. 48, no. 12, pp. 2288–2289, Dec. 2003.

[36] J. Ousingsawat and M. E. Campbell, "Optimal cooperative reconnaissance using multiple vehicles," *J. Guid. Control Dyn.*, vol. 30, no. 1, pp. 122–132, Jan. 2007.

[37] Z. Zhou, B. Yao, R. Xing, L. Shu, and S. Bu, "E-CARP: An energy efficient routing protocol for UWSNs in the Internet of underwater things," *IEEE Sensors J.*, vol. 16, no. 11, pp. 4072–4082, Jun. 2016.

[38] A. Y. Teymorian, W. Cheng, L. Ma, X. Cheng, X. Lu, and Z. Lu, "3D underwater sensor network localization," *IEEE Trans. Mobile Comput.*, vol. 8, no. 12, pp. 1610–1621, Dec. 2009.

[39] N. Saeed, H. Nam, T. Y. Al-Naffouri, and M.-S. Alouini, "A state-of-the-art survey on multidimensional scaling based localization techniques," *IEEE Commun. Surveys Tuts.*, to be published.

[40] A. Vavoulas, H. G. Sandalidis, and D. Varoutas, "Underwater optical wireless networks: A k-connectivity analysis," *IEEE J. Ocean. Eng.*, vol. 39, no. 4, pp. 801–809, Oct. 2014.

[41] V. I. Haltrin, "Chlorophyll-based model of seawater optical properties," *Appl. Opt.*, vol. 38, no. 33, pp. 6826–6832, Nov. 1999.

[42] R. M. Corless, G. H. Gonnet, D. E. G. Hare, D. J. Jeffrey, and D. E. Knuth, "On the Lambert W function," *Adv. Comput. Math.*, vol. 5, no. 1, pp. 329–359, Dec. 1996.
[43] M. Pelka, M. Mackenberg, C. Funda, and H. Hellbruck, "Optical underwater distance estimation," in *Proc. OCEANS Conf.*, Jun. 2017, pp. 1–6.
[44] S. Arnon and D. Kedar, "Non-line-of-sight underwater optical wireless communication network," *J. Opt. Soc. America A*, vol. 26, no. 3, pp. 530–539, Mar. 2009.
[45] H.-R. Fang and D. P. O'Leary, "Euclidean distance matrix completion problems," *Optim. Methods Softw.*, vol. 27, nos. 4–5, pp. 695–717, 2012.
[46] J. R. Martínez-de Dios, A. de San Bernabé-Clemente, A. Torres-González, and A. Ollero, *Cluster-Based Localization and Tracking in Ubiquitous Computing Systems*. Heidelberg, Germany: Springer, 2017.
[47] C. H. Q. Ding, X. He, H. Zha, M. Gu, and H. D. Simon, "A min-max cut algorithm for graph partitioning and data clustering," in *Proc. IEEE Int. Conf. Data Min.*, San Jose, CA, USA, Nov. 2001, pp. 107–114.
[48] S. Ding, L. Zhang, and Y. Zhang, "Research on spectral clustering algorithms and prospects," in *Proc. Int. Conf. Comput. Eng. Technol. (ICCET)*, vol. 6. Chengdu, China, Apr. 2010, pp. 149–153.
[49] N. Saeed, H. Nam, M. I. U. Haq, and D. B. M. Saqib, "A survey on multidimensional scaling," *ACM Comput. Surveys*, vol. 51, no. 3, pp. 1–25, May 2018.
[50] E. G. Larsson, "Cramer–Rao bound analysis of distributed positioning in sensor networks," *IEEE Signal Process. Lett.*, vol. 11, no. 3, pp. 334–337, Mar. 2004.
[51] R. Alghamdi, N. Saeed, H. Dahrouj, M.-S. Alouini, and T. Y. Al-Naffouri, "Towards ultra-reliable low-latency underwater optical wireless communications," in *Proc. IEEE Vehicular Techno. Conf., (VTC)*, Sep. 2019, pp. 1–6.
[52] J. Wang, P. Urriza, Y. Han, and D. Cabric, "Weighted centroid localization algorithm: Theoretical analysis and distributed implementation," *IEEE Trans. Wireless Commun.*, vol. 10, no. 10, pp. 3403–3413, Oct. 2011.

Nasir Saeed (S'14–M'16–SM'19) received the Bachelors of Telecommunication degree from the University of Engineering and Technology, Peshawar, Pakistan, in 2009, the master's degree in satellite navigation from Polito di Torino, Turin, Italy, in 2012, and the Ph.D. degree in electronics and communication engineering from Hanyang University, Seoul, South Korea, in 2015.

He was an Assistant Professor with the Department of Electrical Engineering, Gandhara Institute of Science and IT, Peshawar, from August 2015 to September 2016 and with IQRA National University, Peshawar, from October 2017 to July 2017. He is currently a Postdoctoral Research Fellow with the King Abdullah University of Science and Technology, Thuwal, Saudi Arabia. His current research interests include cognitive radio networks, underwater optical wireless communications, underground communications, dimensionality reduction, and localization.

Mohamed-Slim Alouini (S'94–M'98–SM'03–F'09) was born in Tunis, Tunisia. He received the Ph.D. degree in electrical engineering from the California Institute of Technology, Pasadena, CA, USA, in 1998.

In 2009, he joined the King Abdullah University of Science and Technology, Thuwal, Saudi Arabia, as a Professor of electrical engineering. He served as a Faculty Member with the University of Minnesota, Minneapolis, MN, USA and with Texas A&M University at Qatar, Doha, Qatar. His current research interests include the modeling, design, and performance analysis of wireless communication systems.

Tareq Y. Al-Naffouri (M'10–SM'18) received the B.S. degree (First Class Hons.) in mathematics and electrical engineering from the King Fahd University of Petroleum and Minerals, Dhahran, Saudi Arabia, the M.S. degree in electrical engineering from the Georgia Institute of Technology, Atlanta, Georgia, in 1998, and the Ph.D. degree in electrical engineering from Stanford University, Stanford, CA, USA, in 2004.

He was a Visiting Scholar with the California Institute of Technology, Pasadena, CA, USA, from 2005 to 2006. He was a Fulbright Scholar with the University of Southern California, Los Angeles, CA, USA, in 2008. He has held internship positions with NEC Research Laboratories, Tokyo, Japan, in 1998; the Adaptive Systems Laboratory, University of California at Los Angeles, Los Angeles, in 1999; National Semiconductor, Santa Clara, CA, USA, in 2001 and 2002; and Beceem Communications Santa Clara, in 2004. He is currently an Associate Professor with the Electrical Engineering Department, King Abdullah University of Science and Technology, Thuwal, Saudi Arabia. He has over 240 publications in journals and conference proceedings, 9 standard contributions, 14 issued patents, and 8 pending. His current research interests include sparse, adaptive, and statistical signal processing and their applications, localization, machine learning, and network information theory.

Dr. Al-Naffouri was a recipient of the IEEE Education Society Chapter Achievement Award in 2008 and Al-Marai Award for Innovative Research in Communication in 2009. He has also been serving as an Associate Editor for the IEEE TRANSACTIONS ON SIGNAL PROCESSING since August 2013.